

Rare Kaon Decays

Giuseppina Anzivino*

Department of Physics, University of Perugia, Perugia, Italy

Recent results on charged rare kaon decays from the NA48/2 Collaboration and on neutral kaon decays from the KLOE Collaboration will be reviewed.

I. INTRODUCTION

The results presented in this paper are mainly precision tests of Chiral Perturbation Theory (ChPT), with focus on radiative non-leptonic kaon decays from the NA48/2 and KLOE Collaborations. Semileptonic decays (V_{us} related), leptonic and LFV processes and future rare kaon decays experiments are covered by other talks in these proceedings.

II. NA48/2 - CHARGED KAON DECAYS

The NA48/2 experiment at CERN has taken data in 2003 and 2004 with the main purpose of searching for direct CP violation in the decays of charged kaons into three pions. However, the very high statistics collected, the world's largest, has allowed to study many other decays and to measure their Branching Ratios (BR). In this paper I will focus on radiative nonleptonic decays, that provide a crucial test of the ChPT [1] and can give information on the structure of hadronic interactions at low energy.

A. The NA48/2 experiment

Two simultaneous focused kaon beams of opposite charge, with a central momentum of 60 GeV/c and a momentum band of $\pm 3.8\%$ are produced by a 400 GeV proton beam impinging on a 40 cm Be target. The decay volume is a 114 m long vacuum tank; the final states are reconstructed by a magnetic spectrometer and a liquid krypton calorimeter (LKr). Charged particles are measured by the magnetic spectrometer, consisting of four drift chambers and a dipole magnet located between the second and the third chamber; the momentum resolution is $\sigma(p)/p = 1.02\% \oplus 0.044\%p$ (p in GeV/c). The magnetic spectrometer is followed by a scintillator hodoscope consisting of two planes segmented into horizontal and vertical strips and arranged in four quadrants (charged hodoscope). The electromagnetic Liquid Krypton calorimeter is an almost homogeneous ionization chamber with an active volume of

$\sim 10 m^3$ and a $27 X_0$ thickness; the energy resolution is $\sigma(E)/E = 0.032/\sqrt{E} \oplus 0.09/E \oplus 0.0042$ (E in GeV). The space resolution for single electromagnetic shower can be parametrized as $\sigma_x = \sigma_y = 0.42/\sqrt{E} \oplus 0.06$ cm (E in GeV). At a depth of $\sim 9.5X_0$ inside the active volume of the calorimeter, a hodoscope consisting of a plane of scintillating fibres is installed (neutral hodoscope); the signals from the four quadrants are used to give a fast trigger.

A more detailed description of the detector can be found in [2].

B. The $K^\pm \rightarrow \pi^\pm e^+ e^-$ decay

The $K^\pm \rightarrow \pi^\pm e^+ e^-$ decay is a FCNC process induced at one-loop level in the Standard Model and highly suppressed by the GIM mechanism. The dynamics of the decay is completely specified by the invariant function $W(z)$, where $z = (M_{ee}/M_K)^2$ is a kinematic variable. Several models have been developed predicting the form factors that characterize the decay rate and the dilepton invariant mass distribution. In the present analysis the following parametrizations of the form factors are considered:

- Linear: $W(z) = G_F M_K^2 f_0 (1 + \delta z)$, with free normalization and slope (δz).
- Next-to-Leading Order ChPT [3]: $W(z) = G_F M_K^2 (a_+ + b_+ z) + W^{\pi\pi}(z)$ with free parameters (a_+, b_+) and an explicitly calculated pion loop term $W^{\pi\pi}(z)$.
- A ChPT model developed by a group from Dubna [4] involving meson form factors $W(z) = W(M_a, M_\rho, z)$, with meson masses (M_a, M_ρ) treated as free parameters.

The aim of the analysis is to extract the form factor parameters in the framework of each of the above models and to measure the corresponding BR's in the full kinematic range and, in addition, a model-independent BR in the visible kinematic range ($z > 0.08$). The $K^\pm \rightarrow \pi^\pm e^+ e^-$ rate is measured relatively to $K^\pm \rightarrow \pi^\pm \pi_D^0$ (with $\pi_D^0 \rightarrow e^+ e^- \gamma$). Since the two decays contain the same charged particles in the final state, common selection criteria have been used, resulting in cancelation of particle ID inefficiencies at first order. At the end of the selection, based on the reconstruction of three-track events, a total

*on behalf of the NA48/2 and KLOE Collaborations

of 7146 $K^\pm \rightarrow \pi^\pm e^+ e^-$ candidates with 0.6% background are found in the signal region. The reconstructed ($\pi^\pm e^+ e^-$) invariant mass spectrum is shown in Fig. 1.

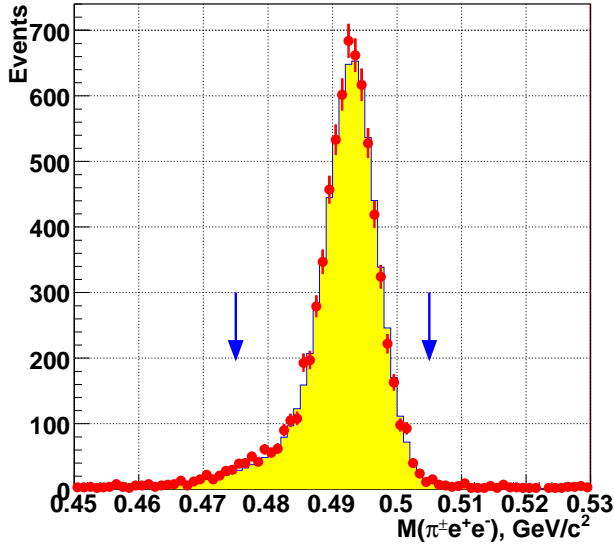


FIG. 1: Reconstructed spectrum of ($\pi^\pm e^+ e^-$) invariant mass: data (dots) and MC simulation (filled area).

The computed values of $d\Gamma_{\pi ee}/dz$ vs z are shown in Fig. 2 with the results of the fits to the three considered models; the measured parameters and the corresponding BR's are presented in Table I.

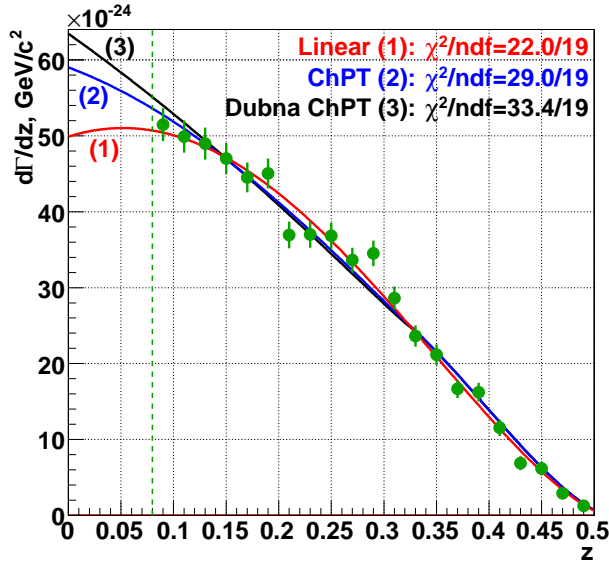


FIG. 2: The computed $d\Gamma_{\pi ee}/dz$ and the results of the fits according to the three considered models.

Fits to all the three models are of reasonable quality, however the linear form-factor model leads to the best χ^2 (see Fig. 2). The data sample is insufficient to

distinguish between the models considered. The BR in the full kinematic range, which includes an uncertainty due to extrapolation into the inaccessible region $z < 0.08$, is

$$BR = (3.08 \pm 0.04_{st.} \pm 0.04_{sys.} \pm 0.08_{ext.} \pm 0.07_{m.}) \times 10^{-7}$$

$$BR(K^\pm \rightarrow \pi^\pm e^+ e^-) = (3.08 \pm 0.12) \times 10^{-7}$$

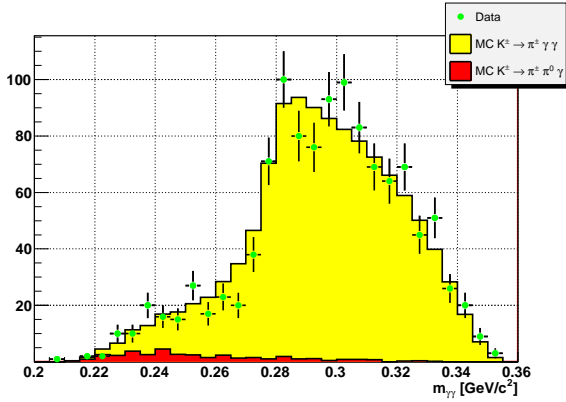
This result is in fair agreement with previous measurements. In particular, comparison to the most precise BNL E865 result [5], dismissing correlated uncertainties due to external BR's and model dependence and using the same external input, reveals a 1.4σ difference. The measurement of δ is in agreement with the previous measurements based on $K^+ \rightarrow \pi^+ e^+ e^-$ [5, 6] and $K^\pm \rightarrow \pi^\pm \mu^+ \mu^-$ [7] samples, and further confirms the contradiction of the data to meson dominance models [8]. The measured f_0 , a_+ and b_+ are in agreement with the only previous measurement [5]. The measured parameters M_a and M_ρ are a few % away from the nominal masses of the resonances [9].

C. The $K^\pm \rightarrow \pi^\pm \gamma \gamma$ decay

The contributions of the chiral lagrangian to this decay [10] appear at $\mathcal{O}(p^4)$, where only the $\Delta I = 1/2$ invariant amplitudes $A(z)$ and $C(z)$, with $z = M_{\gamma\gamma}^2/M_{K^\pm}^2$, contribute. The decay rate and the spectrum strongly depend on a single parameter \hat{c} predicted to be positive and $\mathcal{O}(1)$. The invariant $M_{\gamma\gamma}$ distribution is favored above $2m_{\pi^+}$ and exhibits a cusp at $2m_{\pi^+}$ threshold. Calculations at $\mathcal{O}(p^6)$ [11] show that unitarity correction effects can increase the BR by 30 – 40%, while vector meson exchange contributions would be negligible. The $K^\pm \rightarrow \pi^\pm \gamma \gamma$ decay rate is measured relatively to the $K^\pm \rightarrow \pi^\pm \pi^0$ normalization channel; they have identical particle composition in the final state and only the cut on the $\gamma\gamma$ invariant mass differs for the two channels. About 40% of the total NA48/2 data sample have been analyzed and 1164 candidates have been found with an estimated background of 3.3 % which has to be compared with the only previous experiment [12] that collected 31 events. This decay and the normalization channel were collected through the neutral trigger chain, intended for the collection of $K^\pm \rightarrow \pi^\pm \pi^0 \pi^0$ and therefore suffered from a very low trigger efficiency ($\approx 50\%$). Elaborate studies were performed in order to measure trigger efficiencies and correct for them. The reconstructed invariant $\gamma\gamma$ mass spectrum in the accessible kinematic region is shown in Fig. 3; also shown is the MC expectation assuming the ChPT prediction of $\mathcal{O}(p^6)$ [11]. The model dependent BR of $K^\pm \rightarrow \pi^\pm \gamma \gamma$ has been measured assuming the validity of the $\mathcal{O}(p^6)$ ChPT and $\hat{c} = 2$. The following

TABLE I: Results of fits to the three models and the Model-Independent BR($z > 0.08$).

$\delta =$	$2.35 \pm 0.15_{\text{stat.}} \pm 0.09_{\text{syst.}} \pm 0.00_{\text{ext.}}$	$=$	2.35 ± 0.18
$f_0 =$	$0.532 \pm 0.012_{\text{stat.}} \pm 0.008_{\text{syst.}} \pm 0.007_{\text{ext.}}$	$=$	0.532 ± 0.016
$\text{BR}_1 \times 10^7 =$	$3.02 \pm 0.04_{\text{stat.}} \pm 0.04_{\text{syst.}} \pm 0.08_{\text{ext.}}$	$=$	3.02 ± 0.10
$a_+ =$	$-0.579 \pm 0.012_{\text{stat.}} \pm 0.008_{\text{syst.}} \pm 0.007_{\text{ext.}}$	$=$	-0.579 ± 0.016
$b_+ =$	$-0.798 \pm 0.053_{\text{stat.}} \pm 0.037_{\text{syst.}} \pm 0.017_{\text{ext.}}$	$=$	-0.798 ± 0.067
$\text{BR}_2 \times 10^7 =$	$3.11 \pm 0.04_{\text{stat.}} \pm 0.04_{\text{syst.}} \pm 0.08_{\text{ext.}}$	$=$	3.11 ± 0.10
$M_a/\text{GeV} =$	$0.965 \pm 0.028_{\text{stat.}} \pm 0.018_{\text{syst.}} \pm 0.002_{\text{ext.}}$	$=$	0.965 ± 0.033
$M_\rho/\text{GeV} =$	$0.711 \pm 0.010_{\text{stat.}} \pm 0.007_{\text{syst.}} \pm 0.002_{\text{ext.}}$	$=$	0.711 ± 0.013
$\text{BR}_3 \times 10^7 =$	$3.15 \pm 0.04_{\text{stat.}} \pm 0.04_{\text{syst.}} \pm 0.08_{\text{ext.}}$	$=$	3.15 ± 0.10
$\text{BR}_{\text{MI}} \times 10^7 =$	$2.26 \pm 0.03_{\text{stat.}} \pm 0.03_{\text{syst.}} \pm 0.06_{\text{ext.}}$	$=$	2.26 ± 0.08

FIG. 3: Reconstructed invariant $\gamma\gamma$ mass [GeV/c^2].

preliminary result has been obtained:

$$\text{BR}(K^\pm \rightarrow \pi^\pm \gamma\gamma) = (1.07 \pm 0.04_{\text{stat.}} \pm 0.08_{\text{syst.}}) \times 10^{-6}$$

A model independent BR measurement is in preparation, together with the extraction of \hat{c} from a combined fit of the $m_{\gamma\gamma}$ spectrum shape and the decay rate.

D. The $K^\pm \rightarrow \pi^\pm e^+ e^- \gamma$ decay

The $K^\pm \rightarrow \pi^\pm e^+ e^- \gamma$ decay, observed for the first time by NA48/2, is similar to the $K^\pm \rightarrow \pi^\pm \gamma\gamma$ with one photon internally converting into a $e^+ e^-$ pair. After the basic selection criteria, the data were dominated by $K^\pm \rightarrow \pi^\pm \pi_D^0$ decay, where the π^0 underwent a Dalitz decay $\pi_D^0 \rightarrow e^+ e^- \gamma$. A number of additional selection criteria had to be applied in order to effectively suppress the remaining background due to K^\pm decays and accidental activity. The signal region was defined by requiring $480 < m_{\pi^\pm e^+ e^- \gamma} < 505$ [MeV/c^2]. Since the ChPT predicts only small signal rate and the background increases for low values of $m_{e^+ e^- \gamma}$, the additional requirement $m_{e^+ e^- \gamma} > 0.26$

GeV/c^2 was applied. Using the full NA48/2 data sample, 120 $K^\pm \rightarrow \pi^\pm e^+ e^- \gamma$ (6.1 % background, estimated by MC) candidates are found in the accessible kinematic region.

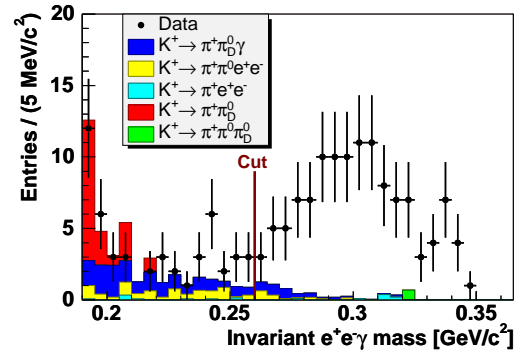
Fig. 4 shows the reconstructed spectrum of $e^+ e^- \gamma$, with the MC expectation for the background contributions. To determine the BR in a model independent way, a partial branching fraction has been computed for each 5 MeV/c^2 wide $m_{e^+ e^- \gamma}$ interval i :

$$\text{BR}_i(K^\pm \rightarrow \pi^\pm e^+ e^- \gamma) = \frac{N_i^{\pi e e \gamma} - N_i^{\text{bkg}}}{A_i^{\pi e e \gamma} \cdot \epsilon} \times \frac{1}{\Phi_K}$$

with $N_i^{\pi e e \gamma}$ and N_i^{bkg} the number of observed signal and estimated background events, $A_i^{\pi e e \gamma}$ the acceptance in bin i . The overall trigger efficiency is ϵ and Φ_K is the total kaon flux. By summing over the bins above $m_{e^+ e^- \gamma} = 0.26 \text{ GeV}/c^2$, the model independent BR is obtained:

$$\begin{aligned} \text{BR}(K^\pm \rightarrow \pi^\pm e^+ e^- \gamma)(M_{e e \gamma} > 0.26 \text{ GeV}/c^2) \\ = (1.19 \pm 0.12_{\text{stat.}} \pm 0.04_{\text{syst.}}) \times 10^{-8} \end{aligned}$$

The parameter \hat{c} has also been measured assuming the validity of $\mathcal{O}(p^6)$ [13]. The final results of the analysis have been recently published [14].

FIG. 4: Reconstructed invariant $e^+ e^- \gamma$ mass [GeV/c^2].

III. KLOE - NEUTRAL KAON DECAYS

The results presented in this section are based on data collected with the KLOE detector at DAΦNE, the Frascati e^+e^- collider operated at a center of mass energy of 1020 MeV, the mass of the ϕ -meson, that is produced almost at rest and decays, in 34% of cases, in $K^0\bar{K}^0$ pairs. The two kaons are always a $K_S K_L$ pure pair, so detection of a K_L guarantees the presence of a K_S . This procedure, called tagging, provides a pure K_S beam.

A. The KLOE detector

The KLOE detector consists of a large cylindrical drift chamber [15] of 4 m diameter and 3.3 m length operated with a low Z and density gas, surrounded by a lead-scintillating fiber calorimeter (EMC)[16]. The chamber provides tracking, measuring momenta with a resolution of $\delta(p_\perp/p_\perp)$ of 0.4% at large angle and a vertex reconstruction resolution of ~ 3.3 mm. A superconducting coil around EMC provides a 0.52 T magnetic field. The EMC is $\sim 15 X_0$ thick and covers 98% of the solid angle. Energy and time resolutions are $\sigma(E)/E = 5.7\%/\sqrt{E}$ and $\sigma(t) = 57$ ps/ $\sqrt{E} \oplus 100$ ps, respectively.

B. The $K_S \rightarrow \gamma\gamma$ decay

The $K_S \rightarrow \gamma\gamma$ decay is an important test of ChPT. The decay amplitude can be calculated unambiguously at the leading $\mathcal{O}(p^4)$ order of the perturbative expansion with an uncertainty of only few percent [17], giving BR ($K_S \rightarrow \gamma\gamma$) = 2.1×10^{-6} .

In the data sample analyzed, corresponding to an integrated luminosity of $\int \mathcal{L} dt \sim 1.9 fb^{-1}$, $\sim 700 \times 10^6$ K_S decays are identified by K_L -tagging. Because of the tagging, no background from $K_L \rightarrow \gamma\gamma$ decay is expected, the main background being $K_S \rightarrow \pi^0\pi^0$, with the two photons undetected, due to geometrical acceptance or non reconstruction in the calorimeter. One of the most effective variables against this kind of background is the arrival time of the photons: a prompt photon is defined as a neutral cluster in the electromagnetic calorimeter satisfying the condition: $|T - R/c| < \min(5 \sigma_t, 2 ns)$, where T is the time of flight, R is the cluster position with respect to the detector origin of the coordinates and σ_t the total time resolution. A signal-enriched sample is defined by requiring two and not more two prompt photons in the event. To maximize $K_S \rightarrow \pi^0\pi^0$ rejection, only clusters with $E > 7$ MeV and $\cos\theta < 0.93$ are considered; the residual background from K_S decays other than $2\pi^0$ is suppressed by vetoing events with photons absorbed in a small angle calorimeter. The event count-

ing is performed using a kinematic fit imposing seven constraints: energy and momentum conservation, the kaon mass and the two photon velocities.

Two other variables with a powerful discrimination against the background are the two photon invariant mass, $M_{\gamma\gamma}$, and the opening angle between the two photons in the K_S center of mass system, $\theta_{\gamma\gamma}^*$. To obtain the number of $K_S \rightarrow \gamma\gamma$ events, a 2 dimensional binned maximum-likelihood of the final sample distribution in the $M_{\gamma\gamma}$ and $\cos\theta_{\gamma\gamma}^*$ variables is performed using the MC generated signal and background shapes, taking into account data and MC statistics. The result of the fit is: $N(\gamma\gamma) = 711 \pm 35$, with $\chi^2/dof = 854/826$, 24.3% CL. Projections of data and fit are shown in Fig. 5. The signal $\cos\theta_{\gamma\gamma}^*$ is peaked at $\cos\theta=-1$, while $M_{\gamma\gamma}$ distribution is gaussian at the K_S mass. The background is less peaked at $\cos\theta=-1$ and shows a broader distribution in mass, populating low mass values. The BR is obtained

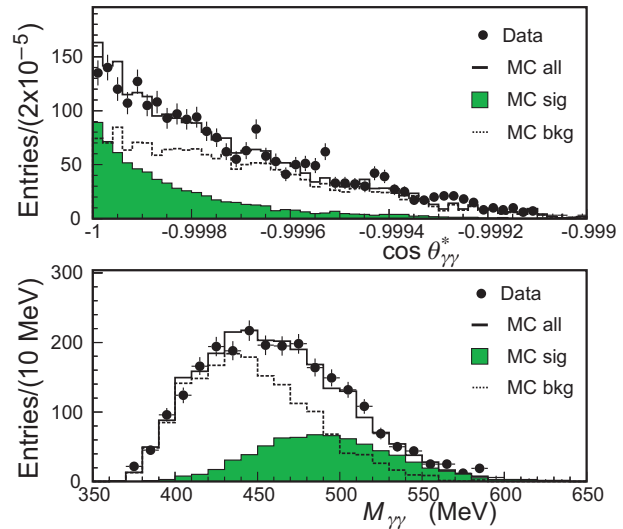


FIG. 5: Distribution of $\cos\theta_{\gamma\gamma}^*$ and $M_{\gamma\gamma}$ for the final sample.

from $N(K_S \rightarrow \gamma\gamma)$ using as normalization channel the $K_S \rightarrow \pi^0\pi^0$ events recorded in the same data sample by counting the K_S tagged events with four prompt photons. The number of $K_S \rightarrow \pi^0\pi^0$ events after correcting for selection efficiency is $(190.5 \pm 0.5) \times 10^6$. Using the latest PDG [9] value for $BR(K_S \rightarrow \pi^0\pi^0) = (30.69 \pm 0.05)\%$, the BR($K_S \rightarrow \gamma\gamma$) is obtained

$$BR(K_S \rightarrow \gamma\gamma) = (2.26 \pm 0.12_{stat.} \pm 0.06_{syst.}) \times 10^{-6}$$

This result together with other existing measurements of $BR(K_S \rightarrow \gamma\gamma)$ as well as the $\mathcal{O}(p^4)$ ChPT theoretical prediction are shown in Fig. 6. There is a 3σ discrepancy between the KLOE result and the NA48 latest measurement [18]: the NA48 measurement implies the existence of a sizable $\mathcal{O}(p^6)$ counterterm in ChPT, while the KLOE result makes this contribution practically negligible.

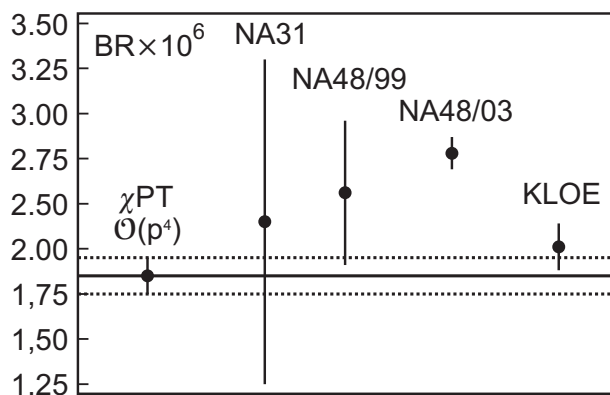


FIG. 6: Comparison of $BR(K_S \rightarrow \gamma\gamma)$ measurements and ChPT predictions.

C. The $K_S \rightarrow e^+e^-$ decay

The decay $K_S \rightarrow e^+e^-$, like $K_L \rightarrow e^+e^-$ and $K_L \rightarrow \mu^+\mu^-$, is a FCNC process suppressed in the SM and dominated by two photon intermediate state. Precise theoretical predictions, based on ChPT at $\mathcal{O}(p^4)$, evaluate the ratio $\Gamma(K_S \rightarrow e^+e^-)/\Gamma(K_S \rightarrow \gamma\gamma) = 8 \times 10^{-9}$ with 10 % uncertainty [19]. Using the present average for $BR(K_S \rightarrow \gamma\gamma) = (2.71 \pm 0.06) \times 10^{-6}$ [9], the SM prediction is $BR(K_S \rightarrow e^+e^-) \sim 10^{-15}$. The best experimental limit has been obtained by the CPLEAR Collaboration [20]: $BR(K_S \rightarrow e^+e^-) < 1.4 \times 10^{-7}$ at 90 % CL. K_S decays are identified by K_L -tagging and selected by requiring two tracks of opposite charge with a good vertex. One of the main backgrounds is the $K_S \rightarrow \pi^+\pi^-$ decay, with two pions misidentified; for these decays the M_{ee} invariant mass is peaked at low values, so a cut at $M_{ee} > 420 \text{ MeV}/c$ is effective in rejecting this type of background. Another important background is the $\phi \rightarrow \pi^+\pi^-\pi^0$ decay with one prompt photon that simulates a K_L interaction in the EMC and the other photon is not detected. After preselection, the data sample is reduced to $\sim 10^6$ events. In order to improve the separation between signal and background, a χ^2 -like variable is defined, using information from the clusters associated to the candidate electron tracks. Using the MC signal events, likelihood variables are built based on: the sum and the difference δt of the two tracks, where $\delta t = t_{cl} - L/\beta c$ is evaluated in the electron hypothesis; the ratio E/p between the cluster energy and the track momentum, for both charges; the cluster position relative to the extrapolation of the track, for both charges. Fig. 7 shows the correlation between χ^2 and M_{ee} for MC signal and background. Two sidebands are defined to check the consistency of MC with data and normalization: region 1 ($M_{ee} < 460 \text{ MeV}/c^2$), dominated by $K_S \rightarrow \pi^+\pi^-$ events, and region 3 ($M_{ee} > 530 \text{ MeV}/c^2$), mostly populated by $\phi \rightarrow \pi^+\pi^-\pi^0$.

A signal box to select $K_S \rightarrow e^+e^-$ events can be conveniently defined in the $\chi^2 - M_{ee}$ plane. Other independent requirements, studied by MC and tuned in the sidebands, have been applied in order to reduce the background contamination, before applying the $\chi^2 - M_{ee}$ selection. The signal box is chosen with an optimization procedure based only on MC. The χ^2 cut for the signal box definition has been chosen to remove all MC background events: $\chi^2 < 70$. The cut on M_{ee} invariant mass is set at $477 < M_{ee} < 510 \text{ MeV}/c^2$, which rules out all signal events with a radiated photon with energy greater than 20 MeV . The signal box selection on data gives $N_{obs} = 0$. The upper limit on $BR(K_S \rightarrow e^+e^-)$ is evaluated using a bayesian approach and normalizing to the number of $K_S \rightarrow \pi^+\pi^-$ events. The result is:

$$BR(K_S \rightarrow e^+e^-) < 9.3 \times 10^{-9} \text{ (90\% CL)}$$

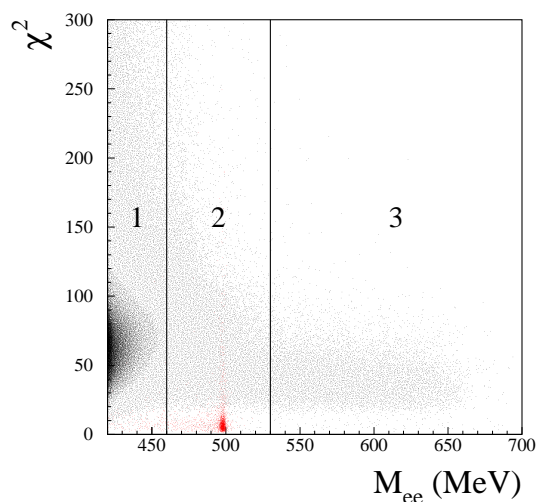


FIG. 7: Distribution of χ^2 as a function of the invariant mass M_{ee} : MC signal (red), background events (black).

This measurement improves by a factor ~ 15 the CPLEAR [20] result and includes for the first time radiative corrections.

D. The $K_L \rightarrow \pi^\pm e^\mp \nu(\gamma)$ decay

The study of radiative K_L decays offers the possibility to obtain information on the kaon structure and to test ChPT. Two different components contribute to the photon emission: the inner bremsstrahlung (IB) and the direct emission (DE). In the $K_{e3\gamma}^0$ decay the IB component is much larger than the DE and the interference terms. It is customary to apply standard cuts to allow comparison among results: $E_\gamma^* > 30 \text{ MeV}$ and $\theta_\gamma^* > 20$ (E_γ^* and θ_γ^* energy and photon angle w.r.t. the lepton in the kaon rest frame, respectively). The

ratio R is defined:

$$R = \frac{\Gamma(K_{e3\gamma}^0; E_\gamma^* > 30 \text{ MeV}, \theta_\gamma^* > 20)}{\Gamma(K_{e3(\gamma)}^0)}$$

Theoretical prediction for R range between 0.95×10^{-2} and 0.97×10^{-2} [21]. The decay amplitude can be written as

$$\frac{d\Gamma}{dE_\gamma^*} \simeq \frac{d\Gamma_{IB}}{dE_\gamma^*} + \langle X \rangle f(E_\gamma^*)$$

where the second term is the SD contribution. All the information on the SD term is contained in the effective strength $\langle X \rangle$. Candidate K_L events are tagged by the presence of a $K_S \rightarrow \pi^+\pi^-$ decay. To count $K_{e3\gamma}^0$ signal events, a two-dimensional fit in the variables $E_\gamma^*, \theta_\gamma^*$ is performed; this allows to measure both R and $\langle X \rangle$. The results of the fit are shown in Fig. 8.

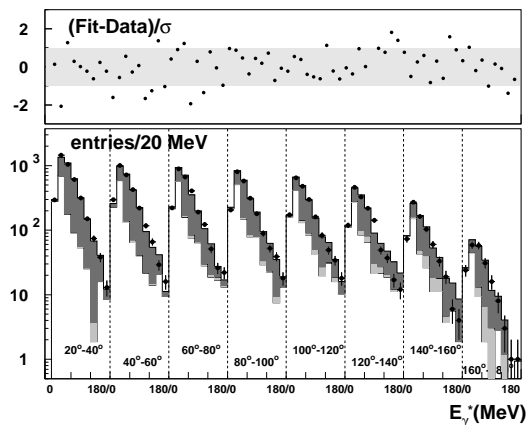


FIG. 8: Fit and fit residuals in bins of E_γ^* .

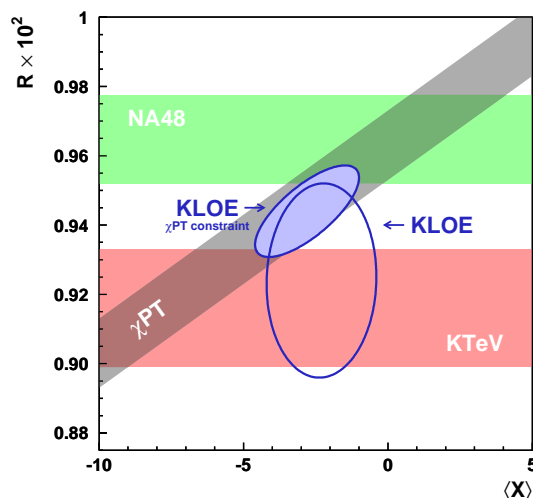


FIG. 9: Comparison of R and $\langle X \rangle$ results (see text).

Taking into account all systematics, the measurement of R and $\langle X \rangle$ yields

$$R = (924 \pm 23_{stat} \pm 16_{syst}) \times 10^{-5}$$

$$\langle X \rangle = -2.3 \pm 1.3_{stat} \pm 1.4_{syst}$$

The measured value of $\langle X \rangle$ is in agreement with $\mathcal{O}(p^6)$ evaluation in [21]. The presence of DE contribution reduces the value of R of about 1%. Fig. 9 shows the comparison of this results with previous measurements. The present accuracy is not sufficient to solve the experimental discrepancy between NA48 [22] and KTeV [23].

-
- [1] G. Ecker, A. Pich, E. de Rafael Nucl. Phys. B **291** (1987) 692.
 - [2] J.R. Batley et al., Phys. Lett. B **634** (2006) 474.
 - [3] G. D'Ambrosio et al., JHEP **8** (1998) 4.
 - [4] A. Z. Dubnickova et al., Phys. Part. Nucl. Lett. **5** vol. 2 (2008) 76.
 - [5] R. Appel et al., Phys. Rev. Lett. **83** (1999) 4482.
 - [6] C. Alliegro et al., Phys. Rev. Lett. **68** (1992) 278.
 - [7] H. Ma et al., Phys. Rev. Lett. **84** (2000) 2580.
 - [8] P. Lichard, Phys. Rev. D **60** (1999) 053007.
 - [9] W.-M. Yao et al. (PDG), J. Phys. G **33** (2006) 1.
 - [10] G. Ecker, A. Pich, E. de Rafael Nucl. Phys. B **303** (1988) 665.
 - [11] G. D'Ambrosio and J. Portoles Nucl. Phys. B **386** (1996) 403.
 - [12] P. Kitching et al. Phys. Rev. Lett. **79** (1997) 4079.
 - [13] F. Gabbiani Phys. Rev. D **59** (1999) 094022.
 - [14] J. R. Batley et al. Phys. Lett. B **659** (2008) 493.
 - [15] M. Adinolfi et al., Nucl. Instr. Methods A **488** (2002) 51.
 - [16] M. Adinolfi et al., Nucl. Instr. Methods A **483** (2002) 689.
 - [17] G. D'Ambrosio and D. Espriu Phys. Lett. B **175** (1986) 237.
 - [18] Kambor Holstein Phys. Rev. D **49** (1994) 2346.
 - [19] NA48 Collaboration, R.J. Batley et al., Phys. Lett. B **551** (2003) 7.
 - [20] G. Ecker, A. Pich Nucl. Phys. B **366** (1991) 189.
 - [21] A. Angelopoulos et al., Phys. Lett. B **413** (1997) 232.
 - [22] J. Gasser et al., Eur. Phys. J. **40** (2005) 205.
 - [23] NA48 Collaboration, A.Lai et al., Phys. Lett. B **605** (2005) 247.
 - [24] KTeV Collaboration, A. Alexopolous et al., Phys. Rev. D **71** (2005) 0122001.